Alqalam Journal of Medical and Applied Sciences. 2025;8(4):2354-2364
https://doi.org/10.54361/ajmas.258437

Original article

A Two-Dimensional Problem with a Gravitational Field and Inclined Load in the Context of Three Thermoelastic Theories

Alzaerah Aldeeb

Department of Mathematics, Faculty of Education, Alzawia University, Libya
Corresponding author.a.aldeeb@zu.edu.ly

Abstract
A model of the equations of two-dimensional problems is studied in a half space, with Porous material under the effect of gravity and an inclined load in the context of the three theories of Lord–Shulman, Green-Lindsay, and classical-coupled. The inclined load is assumed to be a linear combination of a normal mode and a tangential load. The formulation is performed in the context of the Lord-Shulman and Green-Lindsay theories, as well as the classical dynamical coupled theory. Comparisons are made with the results in different values of the angle of inclination, as well as the absence and presence of gravity.
Keywords. Porous Material, Gravity, Inclined load, Lord-Shulman Theory, Green-Lindsay Theory, Normal Mode Analysis.

Introduction

Double-porosity materials, characterized by two well-defined networks of interconnected voids or pores, have attracted significant interest in material science, engineering, and geophysics. These materials possess high permeability and lightweight properties, along with enhanced mechanical performance, making them well-suited for various applications, including energy storage systems, geotechnical engineering, biomedical devices, and advanced composite structures. The coexistence of macroporosity and micro-porosity presents both challenges and opportunities, particularly in understanding their mechanical and thermal behavior within the context of thermoelasticity.
Thermoelasticity theories, which admit a finite speed for thermal signals, have garnered considerable attention over the past four decades. In contrast to the conventional coupled thermoelasticity theory based on a parabolic heat equation,Biot [1], which predicts an infinite speed for the propagation of heat, these theories involve a hyperbolic heat equation. They are referred to as generalized thermoelasticity theories.
Two generalizations to the coupled theory were introduced. The first is ascribed to Lord and Shulman [2] who introduced the theory of generalized thermoelasticity with one relaxation time by postulating a new law of heat conduction to replace the classical Fourier's law. Othman [3] constructed the model of generalized thermoelasticity in an isotropic elastic medium under the dependence of the modulus of elasticity on the reference temperature with one relaxation time.
The second generalization to the coupled theory of thermoelasticity is what is known as the theory of thermoelasticity with two relaxation times, or the theory of temperature rate-dependent thermoelasticity, and was proposed by Green and Lindsay [4]. It is based on a form of the entropy inequality proposed by Green and Laws [5].
The classical theory of elasticity generally disregarded the influence of gravity. Bromwich [6] was the first to explore the impact of gravity on wave propagation in an elastic solid medium. Abo-Dahab et al. [7] examined the Effect of gravity on piezo-thermoelasticity within the dual-phase-lag model. Said et al. [8] have studied the Effect of temperature-dependent properties and gravity on a nonlocal poro-thermoelastic medium with MDD via the G-L Model. Abd Allaand Ahmed [9] investigated the Stoneley and Rayleigh waves in a non-homogeneous orthotropic elastic medium under the influence of gravity. Said and Othman [10] have investigated the 2D problem of a nonlocal thermoelastic diffusion solid with gravity via three theories. Othman et al. [11] studied the Influence of gravity and hall current on a two-temperature fiber-reinforced magneto-visco-thermo-elastic medium using a modified Green-Lindsay model. Kalkal et al. [12] have investigated the Three-phase-lag functionally graded thermoelastic model having double porosity and gravitational effect. Amnah et al. [13] have investigated the effect of gravity on a magneto-thermoelastic porous medium with the framework of a memory-dependent derivative in the context of the 3PHL model. Said [14] studied A viscoelastic-micropolar solid with voids and micro-temperatures under the effect of the gravity field.
The effect of an inclined load on a functionally graded, temperature-dependent thermoelastic material was analyzed by Barak Dhankhar [15]. To examine the thermally insulated stress-free surface of a thermoelastic solid half-space as a result of an inclined load. Othman et al. [16] discussed the effect of gravity and inclined load in a micropolar-thermoelastic medium possessing cubic symmetry under G-N theory. Said. [17] studied the impact of rotation and inclined load on a nonlocal fiber-reinforced thermoelastic half-space via a simple-phase-lag model .Said et al. [18] studied the Effect of an inclined load on a nonlocal fiber-reinforced visco-thermoelastic solid via a dual-phase-lag model. Othman et al. [19], and Sheok et al. [20] on the effects of inclined load on different thermoelastic media. Deswal et al. [21] discussed disturbances in an initially stressed fiber-reinforced orthotropic thermoelastic medium due to an inclined load. A transversely isotropic

***Received**: 15-08-2025 - **Accepted**: 13-10-2025 - **Published**: 22-10-2025*

https://doi.org/10.54361/ajmas.258437

magneto-thermoelastic solid with two temperatures and no energy loss from an inclined load was examined by Lata and Kaur [22]. Alharbi [23] introduced two temperature theories on a micropolar thermoelastic medium with voids under the effect of an inclined load via a three-phase-lag model. In the present work, we shall formulate the generalized thermoelastic medium with a Gravitational Field for three theories with Porous material and inclined load, and solve for the temperature, stress components, and displacement components. The normal method is used to obtain the exact expression for the considered variables. A comparison is carried out between the considered variables as calculated from the generalized thermoelasticity based on L–S, G–L, and coupled theories in the absence and presence of gravity. A comparison is also made between the three theories with different values of the angle of inclination.

Formulation Of the Problem and Basic Equations

We consider a homogeneous isotropic elastic body with voids in a half-space $y \geq 0$ under the effect of a constant gravitational field of acceleration g. Plane strain in the xy -plane with the displacement vector $(u, v, 0)$ such that $u = u(x, y, t)$, $v = v(x, y, t)$. Suppose that an inclined line load f_0 per unit length is acting on the z-axis, and its inclination to the x-axis is θ.

The basic governing equations of a linear thermoelastic medium with voids under the effect of gravity, based on (L-S), (G-L), and coupled theories, are

The stress-strain relation is written as:

$$\sigma_{ij} = [\lambda e_{kk} + b\phi - \beta(1 + \upsilon \frac{\partial}{\partial t})T]\delta_{ij} + \mu e_{ij}, \tag{1}$$

$$e_{ij} = \frac{1}{2}(u_{i,j} + u_{j,i}), \tag{2}$$

The dynamical equations of an elastic medium are given by

$$\mu \nabla^2 u + (\lambda + \mu)\frac{\partial e}{\partial x} + b\frac{\partial \phi}{\partial x} - \beta(1 + v_0 \frac{\partial}{\partial t})\nabla \frac{\partial T}{\partial x} + \rho \, g \frac{\partial v}{\partial x} = \rho \frac{\partial^2 u}{\partial t^2}, \tag{3}$$

$$\mu \nabla^2 v + (\lambda + \mu)\frac{\partial e}{\partial y} + b\frac{\partial \phi}{\partial y} - \beta(1 + v_0 \frac{\partial}{\partial t})\nabla \frac{\partial T}{\partial y} - \rho \, g \frac{\partial u}{\partial x} = \rho \frac{\partial^2 v}{\partial t^2}, \tag{4}$$

The equation of voids is

$$\alpha \nabla^2 \phi - b e - \xi \phi - \omega_0 b \frac{\partial \phi}{\partial t} + m(1 + v_0 \frac{\partial}{\partial t})T = \rho \psi \frac{\partial^2 \phi}{\partial t^2}, \tag{5}$$

The heat conduction equation,

$$K \nabla^2 T = \rho C_E (1 + \tau_0 \frac{\partial}{\partial t})\dot{T} + \beta T_0 (1 + n_0 \tau_0 \frac{\partial}{\partial t})\dot{e} + m \, T_0 (1 + n_0 \tau_0 \frac{\partial}{\partial t})\dot{\phi}. \tag{6}$$

Where σ_{ij} are the components of the stress tensor, e_{ij} are the components of strain, λ, μ are the lame constants, $\beta = (3\lambda + 2\mu)\alpha_t$ such that α_t is the coefficient of thermal expansion, δ_{ij} is the Kronecker delta, $i, j = x, y$. $\alpha, b, \xi, \omega_0, m, \psi$ are the material constants due to the presence of voids? ρ is the density, C_E is the specific heat at constant strain, n_1, n_0 are parameters, τ_0, v_0 are the thermal relaxation times, K is the thermal conductivity, T_0 The reference temperature is chosen so that $|(T - T_0)/T_0| \ll 1$, ϕ is the change in the volume fraction field.

For a two-dimensional problem in the *xy*-plane, Eq. (1) can be written as:

$$\sigma_{ij} = [\lambda(\frac{\partial u}{\partial x} + \frac{\partial v}{\partial y}) + b\phi - \beta(1 + v_0 \frac{\partial}{\partial t})T]\delta_{ij} + \mu(\frac{\partial u}{\partial y} + \frac{\partial v}{\partial x}), \qquad i.j = 1, 2. \tag{7}$$

Consider the following non-dimensional variables:

$$(x', y') = \frac{\omega_1^*}{c_0}(x, y), \; (u', v') = \frac{\omega_1^*}{c_1}(u, v), \; \sigma'_{ij} = \frac{\sigma_{ij}}{\mu}\sigma_{ij}, \; \phi' = \frac{\omega_1^* \chi}{c_1^2}\phi, \; T' = \frac{T}{T_0},$$

$$t' = \omega_1^* t, \; g' = \frac{g}{c_1 \omega_1^*}, \; c_1^2 = \frac{\lambda + 2\mu}{\rho}, \; \omega_1^* = \frac{\rho C_E c_1^2}{k}. v_0' = \omega_1^* v_0, \; \tau_0' = \omega_1^* \tau_0, \tag{8}$$

Using the above non-dimensional variables defined in Eq. (8), the above governing equations take the following form:

$$\nabla^2 u + h_1 \frac{\partial e}{\partial x} + h_2 \frac{\partial \phi}{\partial x} - h_3(1 + v_0 \frac{\partial}{\partial t})\frac{\partial T}{\partial x} + h_4 \frac{\partial v}{\partial x} = h_5 \frac{\partial^2 u}{\partial t^2}, \tag{9}$$

Received: 15-08-2025 - **Accepted**: 13-10-2025 - **Published**: 22-10-2025

$$\nabla^2 v + h_1 \frac{\partial e}{\partial y} + h_2 \frac{\partial \phi}{\partial y} - h_3 (1+v_0 \frac{\partial}{\partial t}) \frac{\partial T}{\partial y} - h_4 \frac{\partial u}{\partial x} = h_5 \frac{\partial^2 v}{\partial t^2}, \tag{10}$$

$$\nabla^2 \phi - h_6 e - h_7 \phi - h_8 \frac{\partial \phi}{\partial t} + h_9 (1+v_0 \frac{\partial}{\partial t}) T = h_{10} \frac{\partial^2 \phi}{\partial t^2}, \tag{11}$$

$$\varepsilon_1 \nabla^2 T - h_{11} (1+ n_0 \tau_0 \frac{\partial}{\partial t}) \frac{\partial \phi}{\partial t} = (1+\tau_0 \frac{\partial}{\partial t}) \frac{\partial T}{\partial t} + \varepsilon_2 (1+ n_0 \tau_0 \frac{\partial}{\partial t}) \frac{\partial e}{\partial t}. \tag{12}$$

Where

$$h_1 = \frac{\lambda+\mu}{\mu}, \quad h_2 = \frac{b c_1^2}{\mu \omega_1^{*2} \psi}, \quad h_3 = \frac{\beta T_0}{\mu}, \quad h_4 = \frac{\rho g c_1^2}{\mu}, \quad h_5 = \frac{\rho c_1^2}{\mu}, \quad h_6 = \frac{b\psi}{\alpha},$$

$$h_7 = \frac{\xi c_1^2}{\alpha \omega_1^{*2}}, \quad h_8 = \frac{\omega_0 c_1^2}{\alpha \omega_1^{*}}, \quad h_9 = \frac{m T_0 \psi}{\alpha}, \quad h_{10} = \frac{\rho c_1^2 \psi}{\alpha}, \quad h_{11} = \frac{m c_1^2}{\rho c e \omega_1^{*2} \psi},$$

$$\varepsilon_1 = \frac{K \omega_1^{*}}{\rho c_1^2 c e}, \quad \varepsilon_2 = \frac{\beta}{\rho c e}.$$

We define displacement potentials R and Q which relate to displacement components u_1 and u_3 as,

$$u = \frac{\partial M}{\partial x} + \frac{\partial Q}{\partial y}, \; v = \frac{\partial M}{\partial y} - \frac{\partial Q}{\partial x}, \tag{13}$$

$$e = \nabla^2 M, \; (\frac{\partial u}{\partial y} - \frac{\partial v}{\partial x}) = \nabla^2 Q. \tag{14}$$

Using Eq. (13) in Eqs. (9)-(12), we obtain:

$$(S_1 \nabla^2 - h_5 \frac{\partial^2}{\partial t^2}) M - h_4 \frac{\partial}{\partial x} Q + h_2 \phi - h_3 (1+v_0 \frac{\partial}{\partial t}) T = 0, \tag{15}$$

$$h_4 \frac{\partial}{\partial x} M + (\nabla^2 - h_5 \frac{\partial^2}{\partial t^2}) Q = 0, \tag{16}$$

$$-h_6 \nabla^2 M + (\nabla^2 - h_7 - h_8 \frac{\partial}{\partial t} - h_{10} \frac{\partial^2}{\partial t^2}) \phi + h_9 (1+v_0 \frac{\partial}{\partial t}) T = 0, \tag{17}$$

$$\varepsilon_2 \frac{\partial^2}{\partial t^2} \nabla^2 M - h_{11} (1+ n_0 \tau_0 \frac{\partial}{\partial t}) \frac{\partial \phi}{\partial t} + \varepsilon_1 \nabla^2 T - (1+\tau_0 \frac{\partial}{\partial t}) \frac{\partial T}{\partial t}. \tag{18}$$

The components of the stress tensor are

$$\sigma_{xx} = h_{12} [\frac{\partial u_1}{\partial x} + \frac{\partial v}{\partial y}] + 2 \frac{\partial u}{\partial x} + h_{13} \phi - h_{14} T, \tag{19}$$

$$\sigma_{yy} = \eta_{12} [\frac{\partial u_1}{\partial x} + \frac{\partial v}{\partial y}] + 2 \frac{\partial v}{\partial z} + \eta_{13} \phi - \eta_{14} T, \tag{20}$$

$$\sigma_{xy} = [\frac{\partial u}{\partial y} + \frac{\partial v}{\partial x}]. \tag{21}$$

Where $(h_{12}, h_{13}, h_{14}, S_1) = (\frac{\lambda}{\mu}, \; \frac{b c_1^2}{\mu \omega_1^{*2} \psi}, \; \frac{\beta T_0}{\mu}(1+v_0 \omega), \; 1+h_1).$

Normal Mode Analysis Method

The solution of the considered physical variable can be decomposed in terms of normal modes in the following form

$$[u, v, M, Q, \phi, T, \sigma_{ij}](x,z,t) = [\bar{u}, \bar{v}, \overline{M}, \bar{\phi}, \bar{T}, \overline{\sigma_{ij}}](y) \exp[i(\omega t + cx)] \tag{22}$$

Where c is the wave number in the x-direction, ω is the complex time constant, $i = \sqrt{-1}$ and $[\bar{u}, \bar{v}, \overline{M}, \bar{\phi}, \bar{T}, \overline{\sigma_{ij}}](y)$ These are the amplitudes of the field quantities.

Using (22) in Eqs. (15)-(18), we obtain

$$(D^2 - S_2) \overline{M} - S_3 \bar{Q} + S_4 \bar{\phi} - S_5 \bar{T} = 0, \tag{23}$$

Received: 15-08-2025 - **Accepted**: 13-10-2025 - **Published**: 22-10-2025

$$S_6\overline{M}+(\mathrm{D}^2-S_7)\,\overline{Q}=0, \tag{24}$$
$$-h_6(\mathrm{D}^2-c^2)R^*+(\mathrm{D}^2-S_8)\overline{\phi}+S_9\overline{T}=0, \tag{25}$$
$$S_{10}(\mathrm{D}^2-c^2)\overline{M}-S_{11}\overline{\phi}+(\mathrm{D}^2-S_{12})\overline{T}=0. \tag{26}$$

Where,

$$(S_2,S_3,S_4,S_5,S_6)=\left(\frac{S_1c^2-h_5\omega^2}{S_1},\ \frac{h_4ic}{S_1},\ \frac{h_2}{S_1},\ \frac{h_3(1+i\,\upsilon\omega)}{S_1},\ h_4ic\right),$$
$$(S_7,S_8,S_9,S_{10})=\left(c^2-h_5\omega^2,\ c^2+h_7+h_8i\,\omega-h_{10}\omega^2,\ h_9(1+i\,\upsilon\omega),\ \frac{-\varepsilon_2(i\,\omega+n_0\tau_0\omega^2)}{\varepsilon_1}\right),$$
$$(S_{11},S_{12})=\left(\frac{h_{11}}{\varepsilon_1},\ \frac{\varepsilon_1c^2+i\,\omega-\tau_0\omega^2}{\varepsilon_1}\right),\quad \mathrm{D}=\frac{\mathrm{d}}{\mathrm{dy}}.$$

Eliminating $\overline{Q}$, $\overline{\phi}$ and T^* between Eqs. (23) - (26), we get the following eighth ordinary differential equation satisfied with $\overline{M}$:

$$[\mathrm{D}^8-A_1\mathrm{D}^6+A_2\mathrm{D}^4-A_3\mathrm{D}^2+A_4]\overline{M}(\mathrm{y})=0. \tag{27}$$

Where

$$A_1=S_{12}+S_8+S_7+S_2-h_6S_4-S_5S_{10},$$
$$A_2=S_8S_{12}+S_9S_{11}+S_7S_{12}+S_7S_8+S_2S_{12}+S_2S_8+S_2S_7+S_6S_3-h_6S_4S_{12}$$
$$-h_6S_4c^2+S_4S_9S_{10}-h_6S_4S_7-h_6S_5S_{11}-S_5S_{10}c^2-S_5S_8S_{10}-S_5S_7S_{10},$$
$$A_3=S_7S_8S_{12}+S_7S_9S_{11}+S_2S_8S_{12}+S_2S_9S_{11}+S_2S_7S_{12}+S_2S_7S_8+S_3S_6S_{12}+S_3S_6S_8$$
$$+h_6S_4S_{10}c^2+S_4S_9S_{10}c^2-h_6S_4S_7S_{12}-h_6S_4S_7c^2+S_4S_7S_9S_{10}-h_6S_5S_{11}c^2$$
$$-S_5S_8S_{10}c^2-h_6S_5S_7S_{11}-S_5S_7S_{10,}c^2-S_5S_7S_8S_{10},$$
$$A_4=S_2S_7S_8S_{12}+S_2S_7S_9S_{11}+S_3S_6S_8S_{12}+S_3S_6S_9S_{11}-h_6S_4S_7S_{12}c^2+S_4S_7S_9S_{10}c^2$$
$$-h_6S_5S_7S_{11}c^2-S_5S_7S_8S_{10}c^2.$$

In a similar manner, we get

$$[\mathrm{D}^8-A_1\mathrm{D}^6+A_2\mathrm{D}^4-A_3\mathrm{D}^2+A_4]\{\overline{M}(\mathrm{y}),\overline{Q}(\mathrm{y}),\overline{\phi}(\mathrm{z}),\overline{T}(\mathrm{y})\}=0. \tag{28}$$

Equation (28) can be factored as

$$[(\mathrm{D}^2-k_1^2)(\mathrm{D}^2-k_2^2)(\mathrm{D}^2-k_3^2)(\mathrm{D}^2-k_4^2)]\{\overline{M}(\mathrm{y}),\overline{Q}(\mathrm{z}),\phi^*(\mathrm{y}),\overline{T}(\mathrm{y})\}=0. \tag{29}$$

Where $k_n^2\,(n=1,2,3,4)$ are the roots of the equation (28).

The solution of equation (28), which is bounded as $y\rightarrow\infty$, is given by:

$$\overline{M}=\sum_{n=1}^{4}R_ne^{-k_ny}, \tag{30}$$
$$\overline{Q}=\sum_{n=1}^{4}L_{1n}R_ne^{-k_ny}, \tag{31}$$
$$\overline{\phi}=\sum_{n=1}^{4}L_{2n}R_ne^{-k_ny}, \tag{32}$$
$$\overline{T}=\sum_{n=1}^{4}L_{3n}R_ne^{-k_ny}. \tag{33}$$

Where, $R_n\ (n=1,2,3,4)$ are constants.

To obtain the components of the displacement vector from (30) and (33) in (13)

$$\overline{u}=\sum_{n=1}^{4}L_{4n}R_ne^{-k_ny} \tag{34}$$
$$\overline{v}=\sum_{n=1}^{4}L_{5n}R_ne^{-k_ny}, \tag{35}$$

From Eqs. (32)-(35) in (19)-(21) to obtain the components of the stresses

Received: 15-08-2025 - **Accepted**: 13-10-2025 - **Published**: 22-10-2025

https://doi.org/10.54361/ajmas.258437

$$\overline{\sigma_{xx}} = \sum_{n=1}^{4} L_{6n} R_n e^{-k_n y}, \tag{36}$$

$$\overline{\sigma_{yy}} = \sum_{n=1}^{4} L_{7n} R_n e^{-k_n y}, \tag{37}$$

$$\overline{\sigma_{xy}} = \sum_{n=1}^{4} L_{8n} R e^{-k_n y}. \tag{38}$$

Where,

$$L_{1n} = \frac{-S_6}{(k_n^2 - S_7)},\ L_{2n} = \frac{-[-h_6 S_5(k_n^2 - c^2) + S_9(k_n^2 - S_2 - S_3 L_{1n}]}{[S_5(k_n^2 - S_8) + S_4 S_9]},\ L_{3n} = \frac{k_n^2 - S_2 - S_3 L_{1n} + S_4 L_{2n}}{S_5},$$

$$L_{4n} = ic - k_n L_{1n},, \quad L_{5n} = -(k_n + icL_{1n}),$$

$$L_{6n} = h_{12}(icL_{4n} - k_n L_{5n}) + 2icL_{4n} + h_{13}L_{2n} - h_{14}L_{3n},$$

$$L_{7n} = h_{12}(icL_{4n} - k_n L_{5n}) - 2k_n L_{5n} + h_{13}L_{2n} - h_{14}L_{3n},\ L_{8n} = (-k_n L_{4n} + icL_{5n}).$$

The Boundary Conditions of The Problem

We consider an inclined load P acting in the direction that makes an angle θ with the direction of the x-axis:

$$\frac{\partial T}{\partial y} = 0,\ \sigma_{yy} = F_1 e^{i(\omega t + ax)} = -(\mathrm{P}\cos\theta) e^{i(\omega t + ax)},\ \sigma_{xy} = F_2 e^{i(\omega t + ax)} = -(\mathrm{P}\sin\theta) e^{i(\omega t + ax)},$$

$$\frac{\partial \phi}{\partial y} = 0, \tag{39}$$

By inserting Eqs. (32-33) and (36)-(38) into Eq. (39), we have

$$\sum_{n=1}^{4} L_{3n} R_n = 0,\ \sum_{n=1}^{4} L_{7n} R_n = -\mathrm{P}\cos\theta,\ \sum_{n=1}^{4} L_{8n} R_n = -\mathrm{P}\sin\theta,\ \sum_{n=1}^{4} -k_n L_{2n} R_n = 0. \tag{40}$$

Solving the above system of equations (40), we obtain a system of four equations. After applying the inverse matrix method, we have the values of the four constants. Hence, we obtain the expressions of displacements, temperature distribution, and the stress components:

$$\begin{pmatrix} R_1 \\ R_2 \\ R_3 \\ R_4 \end{pmatrix} = \begin{pmatrix} L_{31} & L_{32} & L_{33} & L_{34} \\ L_{71} & L_{72} & L_{73} & L_{74} \\ L_{81} & L_{82} & L_{83} & L_{84} \\ -k_1 L_{21} & -k_1 L_{22} & -k_1 L_{23} & -k_1 L_{24} \end{pmatrix}^{-1} \begin{pmatrix} 0 \\ -P\cos\theta \\ -P\sin\theta \\ 0 \end{pmatrix}. \tag{41}$$

Numerical Results

In order to illustrate the obtained theoretical results in the preceding section, following Dhaliwal and Singh in (1980), the magnesium material was chosen for purposes of numerical evaluations. The constants of the problem were taken as

$$\lambda = 2.14\times10^{10}\ N/.m^2,\ \mu = 3.278\times10^{10}\ N/m^2,\ K = 1.7\times10^2 W/m\deg,\ \alpha_t = 1.78\times10^{-5} N/m^2,$$

$$\rho = 1.74\times10^3\ Kg/.m^3,\ C_E = 1.04\times10^3\ J/Kg\deg,$$

$$T_0 = 298\,K,\ \beta = 2.68\times10^6 N/m^2\deg,\ \omega_1^* = 3.58\times10^{11}/s.$$

The void parameters are

$$\chi = 1.753\times10^{-15} m^2,\ \xi = 1.475\times10^{10} N/m^2,\ b = 1.13849\times10^{10} N/m^2,$$

$$\alpha = 3.688\times10^{-5} N,\ m = 2\times10^6 N/m^2\deg,\ \omega_0 = 0.0787\times10^{-3} N/m^2 s.$$

The comparisons were carried out for

$$x = 0.5,\ t = 0.1,\ c = -1,\ \omega = \zeta_0 + i\zeta_1,\ \zeta_0 = -1,\ \zeta_1 = -1,\ P = -0.9\ \theta = 60^\circ,$$

$$f = 1,\ \tau_0 = 1\,s,\ \upsilon = 1.5\,s,\ 0 \le y \le 6.$$

The above numerical technique was used for the distribution of the real parts of the displacement components u and v, the temperature T, the stress components σ_{xx}, σ_{yy} and σ_{xy} and a change in the volume fraction field ϕ with the distance y for the problem under consideration. in 2D for three different theories of thermoelasticity (CD, L-S, and G-L). All the physical quantities are shown graphically in Figures 1-6 in the case of two different values of the gravity effect $(g = 0,\ g = 9.8)$ at $\theta = 60^\circ$.

Received: *15-08-2025* - ***Accepted***: *13-10-2025* - ***Published***: *22-10-2025*

https://doi.org/10.54361/ajmas.258437

(Figure 1) illustrates the variation of the vertical displacement u under two scenarios: with and without gravity. We notice that displacement u for case $g = 0$ of the three theories begins fromnegative values, and begins from positive values in the case of $g = 9.8$ in the context of the three theories (CD), (L-S), and (G-L). The values of the horizontal displacement u are decreasingin the range $0 \le y \le 1$, then increasingin the range for $g = 0$, and the values of the horizontal displacement u for $g = 9.8$ start decreasing in the range $0 \le y \le 0.7$, then increasing in the range $0.7 \le y \le 6$ for the three theories. (Figure 2) presents the variation of the horizontal displacement v as a function of the spatial or temporal variable, comparing two different cases: the presence and the complete absence of gravity. The values of the distribution of the vertical displacement v begins from positive values with gravity inthe context of the three theories, and starts from in the range $0 \le y \le 1.3$, are increasing and decreasing from the range $1.3 \le y \le 3$, and decreasing from the range and increasing from the range $3 \le y \le 6$ from three theories. We notice that theories of the values of the horizontal displacement v without gravity are large compared to the values of v with gravity, for the three theories (Figure 3). The temperature distribution T is plotted for both the presence and absence of gravity. The distribution of the temperature T is initiated with a non-negative value that obeys the boundary conditions in the absence and presence of gravity for three theories. When a gravitational field exists, T increases for $0 \le y \le 0.8$, and decreasing from $0.8 \le y \le 6$ for three theories. (Figure 4) displays the variation in the volume fraction field ϕ which starts at zero value with gravity, verifies the boundary condition, and the volume fraction field ϕ always begin from positive values in the absence of gravityin the three theories. The values of ϕ are increasing to a maximum value in the range $0 \le y \le 0.5$, then decreasing in the range, and increasing from the range $1.7 \le y \le 6$ from three theories. (Figure 5) clarifies the distribution of the normal stress σ_{yy} versus the distance y. It is clear that the gravity stress component increases with the increase of σ_{yy}. The values of σ_{yy} begins from negative values (which is the same point) for both the presence and absence of gravity in the context of the three theories. It is observed that the distribution of the stress component σ_{yy} The gravity is greater than that without gravity. (Figure 6) exhibits that the distribution of the stress component σ_{xy}, begins from a negative value in the case of (g=0, g=9.8) under the three theories, and satisfies the boundary conditions at $y = 0$.

Similarly, the distributions of the real parts of the above physical quantities with distance y In 2D, for three theories with inclined effect are shown graphically in Figures 7-11 in the case of different values of angle (θ = 15°, 45°) at g=9.8. Figure 7 explains the distribution of the displacement components v in the case of (θ = 15°, 45°) and in the context of (CD), (L-S), and (G-L). The distribution of v is increasing with the increase of θ. (Figure 8) investigated the variation of the temperature distribution T, with distance y. It is observed that the distribution of T increases with the increase of θ under the three theories for $y > 0$. (Figure 9) depicts the distribution of the change in the volume fraction field ϕ increases with the increase of θ. (Figure 10) demonstrates that the distribution of c σ_{yy} in the case of (θ= 15°, 45°) increases with the increase of θ. (Figure 11) depicts the distribution of the distribution of stress component σ_{xy} under the three theories, begins from a positive value in the case of (θ= 15°, 45°), and satisfies the boundary conditions at $y = 0$.

3D variations represent the complete relations between the displacement components u,v, also stress components σ_{yy} ,σ_{xy}, and both components of distance as shown in Figures 12-15, in the presence of the gravity field g=9.8 at 45°in the context of (G-L) theory. These figures are very important to study the dependence of these physical quantities on the two displacement components. The curves obtained are highly dependent on the distance from the origin; all the physical quantities are moving in wave propagation.

***Received**: 15-08-2025 - **Accepted**: 13-10-2025 - **Published**: 22-10-2025*

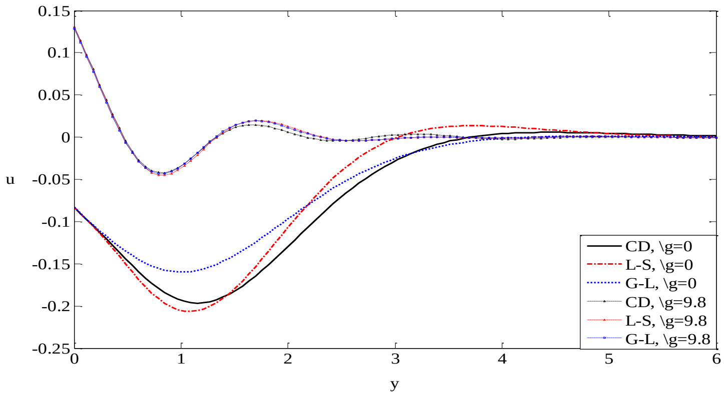

Fig 1. Variation of the horizontal displacement u he presence and complete absence of gravity

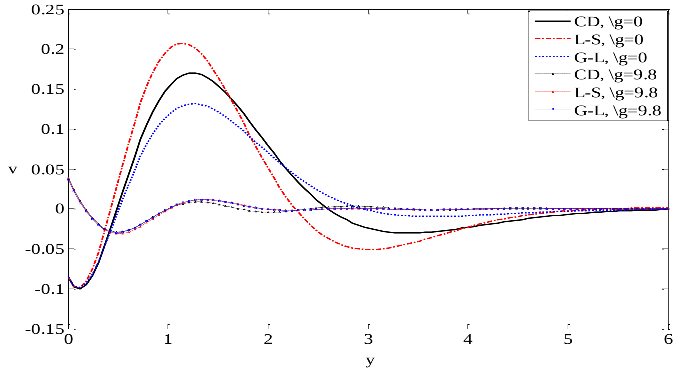

Fig 2. Variation of the horizontal displacement with the presence and complete absence of gravity

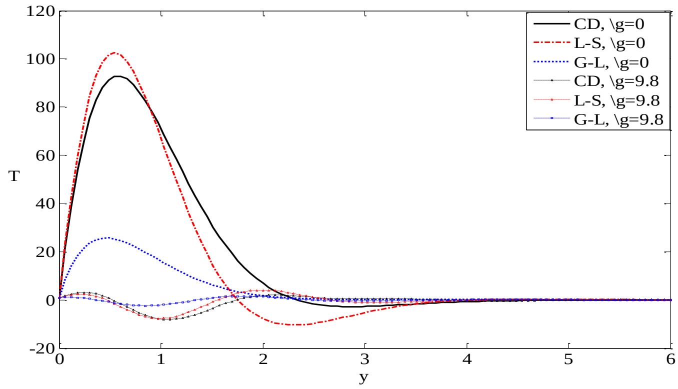

Fig. 3 variation of the temperature Tin the presence and complete absence of gravity

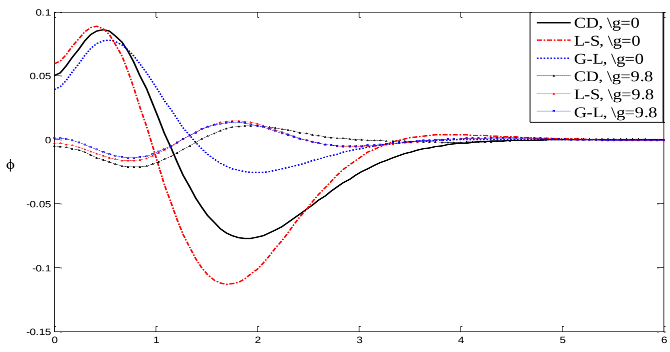

Fig.4 Change in volume fraction field distribution in the presence and complete absence of gravity

***Received**: 15-08-2025 - **Accepted**: 13-10-2025 - **Published**: 22-10-2025*

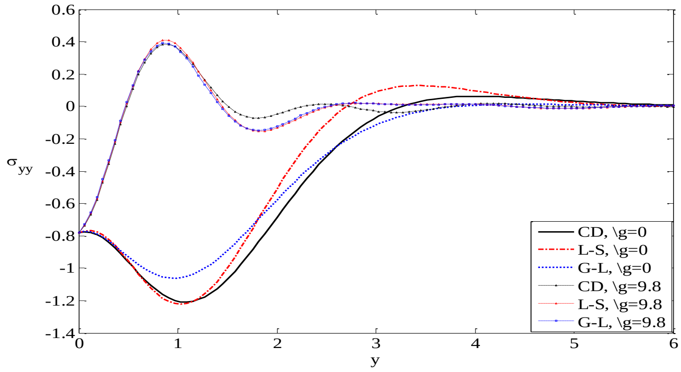

Fig.5. Variation of the force stress components σ_{yy} in the presence and complete absence of gravity

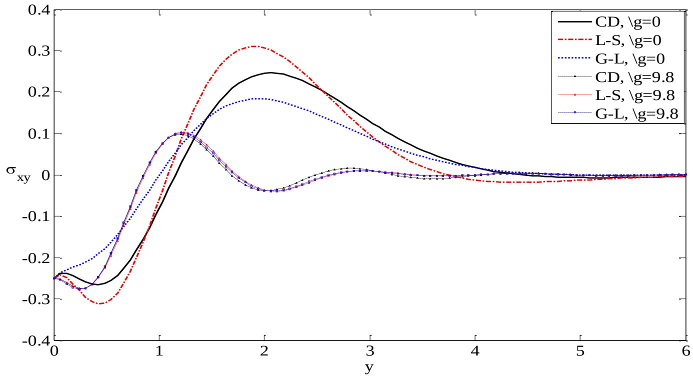

Fig. 6 Variation of the force stress components σ_{xy} in the presence and complete absence of gravity

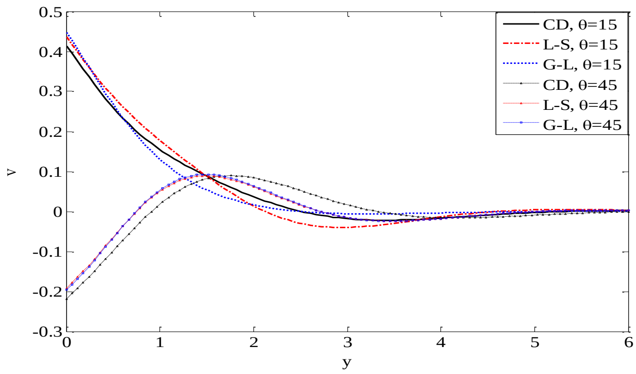

Fig. 7. Vertical displacement distribution v in the different values of θ

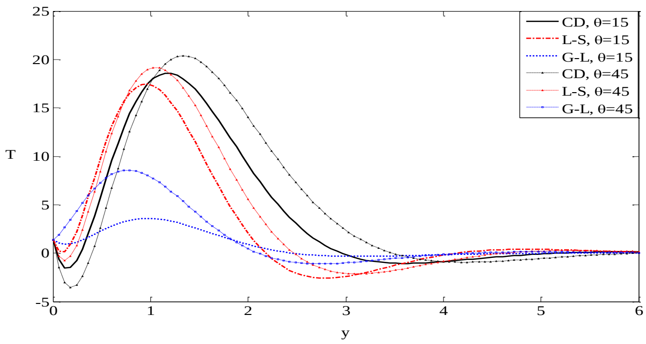

Fig. 8. Temperature distribution Tin the different values of θ

***Received**: 15-08-2025 - **Accepted**: 13-10-2025 - **Published**: 22-10-2025*

Alqalam Journal of Medical and Applied Sciences. 2025;8(4):2354-2364
https://doi.org/10.54361/ajmas.258437

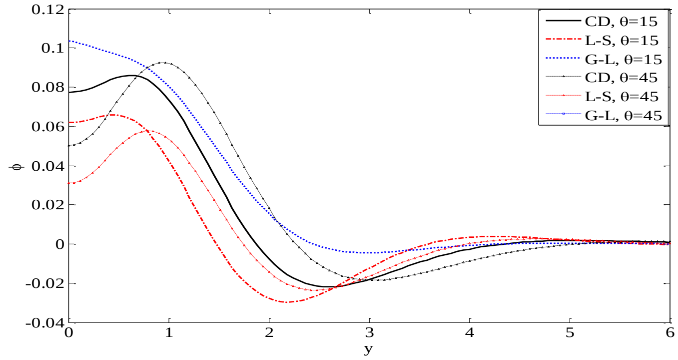

Fig.9. Distribution of the temperature function ϕ in the different values of θ

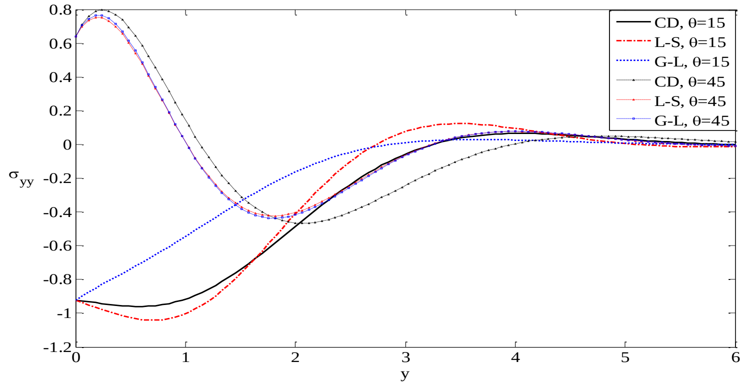

Fig. 10. The distribution of the stress component σ_{yy} in the different values of θ

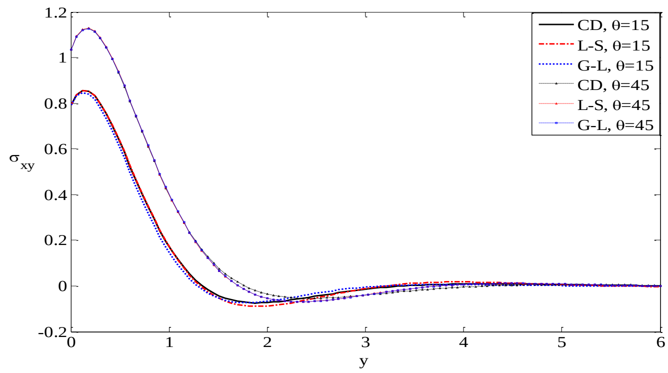

Fig. 11. The distribution of stress componentsσ_{xy} in the different values of θ

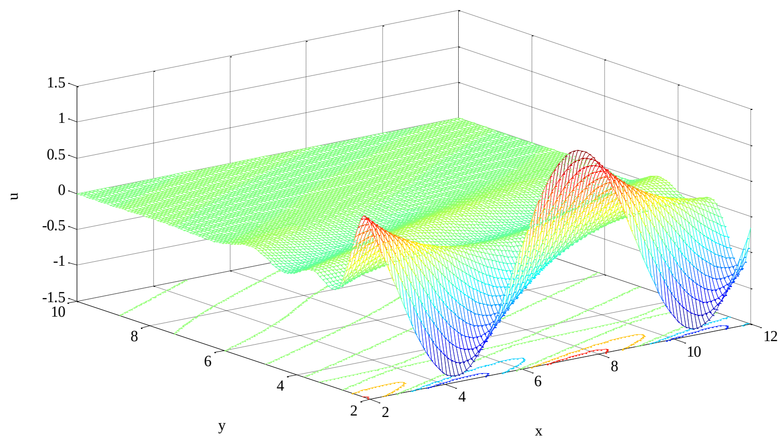

Fig. 12. 3D variation of the displacement u with the variation of x, y under (G-L) theory

***Received**: 15-08-2025 - **Accepted**: 13-10-2025 - **Published**: 22-10-2025*

https://doi.org/10.54361/ajmas.258437

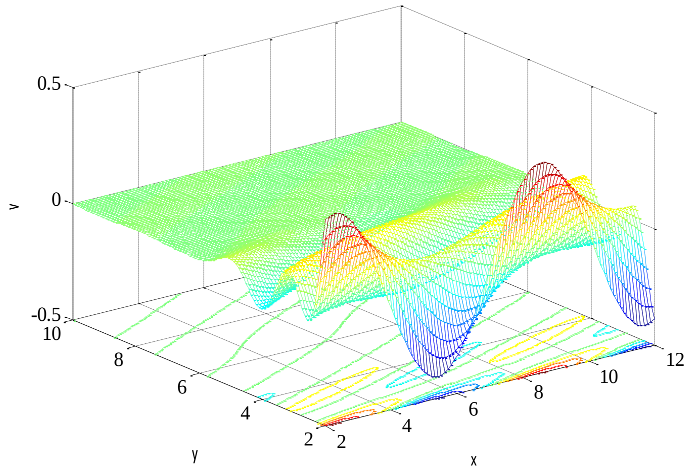

Fig. 13. 3D variation of the displacement v with the variation of x, y under (G-L) theory

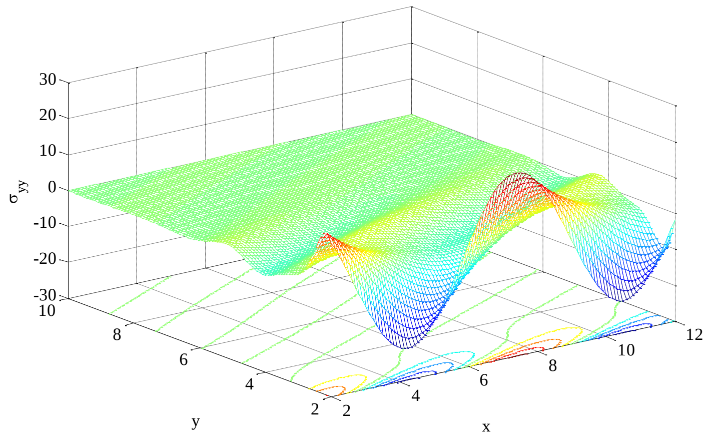

Fig. 14. 3D variation of the street σ_{yy} ***with the variation of x, y under (G-L) theory***

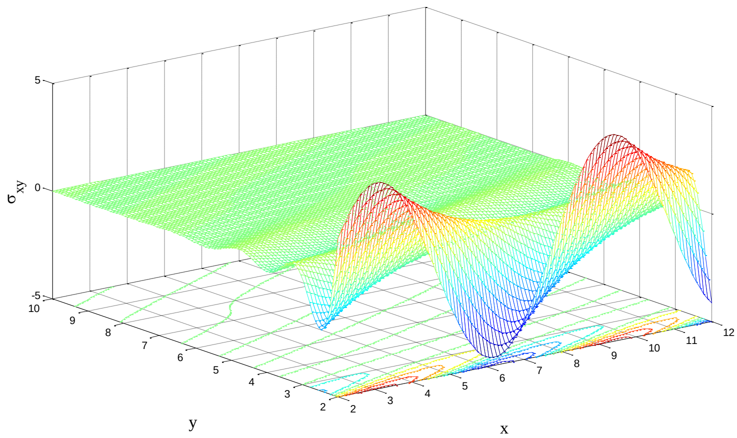

Fig. 15. 3D variation of the street σ_{xy} ***with the variation of x, y under (G-L) theory***

Conclusion

The paper emphasized studying how the influence of thermal memory varies while considering the three theories. The application of normal model analysis leads to the development and utilization of analytical solutions for the thermoelastic problem in solids. The values of all the physical quantities converge to 0 by increasing the distance y and all the functions are continuous. The gravity field and the inclined load play a significant role in the distribution of all the physical quantities.

References

1. Biot MA. Thermoelasticity and irreversible thermodynamics. J Appl Phys. 1956;27:240-253.
2. Lord HW, Shulman Y. A generalized dynamical theory of thermoelasticity. J Mech Phys Solids. 1967;15:299-306.

Received*: 15-08-2025 -* ***Accepted****: 13-10-2025 -* ***Published****: 22-10-2025*

3. Othman MIA. Lord-shulman theory under the dependence of the modulus of elasticity on the reference temperature in two dimensional generalized thermo-elasticity. J Therm Stresses. 2002;25(10):1027-1045.
4. Green AE, Lindsay KA. Thermoelasticity. J Elasticity. 1972;2(1):1-7.
5. Green AE, Laws N. On the entropy production inequality. Arch Ration Mech Anal. 1972;45:47-53.
6. Bromwich TJI. On the influence of gravity on elastic waves, and, in particular, on the vibrations of an elastic globe. Proc Lond Math Soc. 1898;30(1):98-120.
7. Abo-Dahab SM, Bayones FS, Alharbi FM, Abd-Alla AM, Aljohani AF, Kilany AA. Magneto-thermoelastic surface waves phenomenon with voids, gravity, initial stress, and rotation under four theories. Alex Eng J. 2024;105:743-759.
8. Said SM, Othman MIA, Eldemerdash MG. Effect of temperature-dependent properties and gravity on a nonlocal poro-thermoelastic medium with MDD via G-L Model. J Vib Eng Technol. 2025;13:116.
9. Abd-Alla AM, Ahmed SM. Stoneley and Rayleigh waves in a non-homogeneous orthotropic elastic medium under the influence of gravity. J Appl Math Comput. 2003;135(1):187-200.
10. Said SM, Othman MIA. 2D problem of a nonlocal thermoelastic diffusion solid with gravity via three theories. J Vib Eng Technol. 2024;12:5423-5430.
11. Othman MIA, Said SM, Gamal EM. Influence of gravity and hall current on a two-temperature fiber-reinforced magneto-visco-thermo-elastic medium using a modified Green-Lindsay model. Mech Solids. 2023;58(9):3428-3447.
12. Kalkal KK, Kadian A, Kumar S. Three-phase-lag functionally graded thermo-elastic model having double porosity and gravitational effect. J Ocean Eng Sci. 2023;8(1):42-54.
13. Alharbi AM, Said SM, Othman MIA. Effect of gravity on a magneto-thermoelastic porous medium with the frame of a memory-dependent derivative in the context of the 3PHL model. Steel Compos Struct. 2021;40(6):881-891.
14. Said SM. A viscoelastic-micropolar solid with voids and micro-temperatures under the effect of the gravity field. Geomech Eng. 2022;31(2):159-166.
15. Barak MS, Dhankhar P. Effect of inclined load on a functionally graded fiber-reinforced thermoelastic medium with temperature-dependent properties. Acta Mech. 2022;233:3645-3662.
16. Othman MIA, Abo-Dahab SM, Alosaimi HA. The effect of gravity and inclined load in micropolar thermoelastic medium possessing cubic symmetry under G-N theory. J Ocean Eng Sci. 2018;3(4):288-294.
17. Said SM. The impact of rotation and inclined load a nonlocal fiber-reinforced thermoelastic half-space via simple-phase-lag model. J Vib Eng Technol. 2024; [Epub ahead of print].
18. Said SM, Othman MIA, Gamal EM. Effect of an inclined load on a nonlocal fiber-reinforced visco-thermoelastic solid via a dual-phase-lag model. 2024; [Epub ahead of print].
19. Othman MIA, Alosaimi H, Abd-Elaziz EM. Effect of initial stress and inclined load on generalized micropolar thermoelastic medium possessing cubic symmetry with three-phase-lag model. Mech Solids. 2023;58(12):2333-2348.
20. Sheokand P, Deswal S, Punia BS. Influence of variable thermal conductivity and inclined load on a nonlocal photo-thermoelastic semiconducting medium with two temperatures. J Therm Stresses. 2024;47(2):217-239.
21. Deswal S, Poonia R, Kalkal KK. Disturbances in an initially stressed fiber-reinforced orthotropic thermoelastic medium due to inclined load. J Braz Soc Mech Sci Eng. 2020;42:261.
22. Lata P, Kaur I. Effect of rotation and inclined load on transversely isotropic magneto thermoelastic solid. Struct Eng Mech. 2019;70(2):245-255.
23. Alharbi AM. Two temperature theory on a micropolar thermoelastic media with voids under the effect of inclined load via three-phase-lag model. Z Angew Math Mech. 2021;101(12):e202100078.

***Received**: 15-08-2025 - **Accepted**: 13-10-2025 - **Published**: 22-10-2025*